Materials Research Proceedings 33 (2023) 388-396 https://doi.org/10.21741/9781644902677-57

High-fidelity simulation of shock-wave/boundary layer interactions

A. Ceci

Sapienza University of Rome, Department of Mechanical and Aerospace Engineering, via Eudossiana 18, Rome 00184

alessandro.ceci@uniroma1.it

Keywords: Compressible Boundary Layers, Shock Waves, Turbulence Simulation

Abstract. We perform direct numerical simulations of impinging shock-boundary layer interaction on a flat plate, in which the shock is not orthogonal to the boundary layer flow. The analysis relies on an idealized configuration, where a spanwise flow component is used to introduce the effect of the sweep angle between a statistically two-dimensional boundary layer and the shock. A quantitative comparison is carried out between the swept case and the corresponding unswept one, and the effect of the domain spanwise width is examined. The analysis reveals that, while the time-averaged swept flow characteristics are basically unaffected by the choice of the domain width, the spectral dynamics of the flow dramatically changes with it. For very narrow domains, a pure two-dimensional, low-frequency component can be detected, which resembles the low-frequency oscillation of the unswept case. The present work is also devoted to compare the performance of Digital Filtering (DF) and Recycling-Rescaling methods (RR) in reaching an equilibrium state for the Direct Numerical Simulation (DNS) of a turbulent boundary layer. We performed two sets of DNS of supersonic and hypersonic boundary layers, based on previous numerical studies. It is found that, overall, the RR method is the most appropriate choice, to quickly reach a correct trend of the wall pressure fluctuations, whereas the DF method is more capable in obtain small deviations of the skin friction coefficient with respect to the benchmark.

Introduction

Shock-wave/turbulent-boundary-layer interactions (SBLIs) are encountered in a multitude of aeronautics and aerospace applications. Interactions of this kind frequently occur in external flows, owing to aerodynamic interference between aircraft appendices/boosters and main body, as well as internal flows, for instance air intakes. More generally, SBLIs are found whenever a shock wave sweeps across a turbulent boundary layer developing on a solid surface. The presence of SBLI may lead to significant drawback on aerodynamic performance of aircraft, yielding loss of efficiency of the aerodynamic surfaces, unwanted wall pressure fluctuations possibly leading to structural vibrations, and localized heat transfer peaks, especially when extensive flow separation occurs [3],[9],[13]. The present work focuses on the study of these interactions when the boundary layer upstream of the shock impingement is in the turbulent regime, using direct numerical simulations.

Most available works on turbulent SBLI [19],[21],[23],[24],[25] focus on simplified configurations in which the shock is perfectly orthogonal to the main stream. A peculiar aspect of this kind of interactions is the coupling of the separation flow with the turbulent structures in the upcoming boundary layer, which locally modifies the shear layer embedded in the separation bubble, generating low-frequency oscillation of the separated region [19],[25]. This mechanism yields intense low-frequency tones in the temporal spectrum of the wall pressure fluctuations, whose prediction is important for the safety and integrity of aircraft structures.

Engineering applications, however, often feature more geometrically complex interactions, in which the shock impingement line is not orthogonal to the incoming flow. This is the case of fully three-dimensional SBLIs, whose prototypes are flows over swept compression ramps

[10],[28],[33],[34] and around fins [14],[27]. These interactions are made more complicated from the presence of a cross-flow with respect to the shock impingement lines, and by the fact that the separation bubble (when present) is of open type as contrasted to the case of 3D interactions in which separation streamlines must be closed. It is now established that, depending on relative strength of the incoming shock, the near-wall interaction region may have either cylindrical symmetry (namely, the size does not vary along the span) in the case of weak-to-mild interactions, or conical symmetry with length scale linearly increasing along the span in the case of strong interactions [29],[32]. Shock skewing is known to modify the frequency and the intensity of the wall pressure fluctuations, depending on the flow sweep angle [10] also by introducing cross-flow instabilities within the separation bubble [33]. Owing to greater geometrical complexity and difficulty to get converged statistics, three-dimensional SBLIs have been addressed in a much more limited number of studies than their two-dimensional counterparts ([1],[2],[12],[39]).

Researchers have recently attempted to overcome the complexity of three-dimensional SBLI investigations by considering simple geometries able to mimic at least part of the typical phenomena arising in the aforementioned applications. The arguably simplest configuration which can be used at this aim is the interaction between a swept oblique shock wave and a fully developed flat plate boundary layer. Both experimental [18] and numerical works [15] have been recently published using this approach: the former study used a swept shock generator to introduce a shock wave that is not orthogonal to the boundary layer mean flow direction, whereas the aforementioned numerical investigation employs a swept inflow condition for the boundary layer to generate a three-dimensional interaction.

A critical ingredient in the numerical setup of DNS of spatially developing flows is the choice of the inflow conditions. In fact, it is now known that both inflow mean velocity profile [1] and the velocity fluctuations [7] may affect the statistical properties of DNS. The data scatter between simulations with the same free-stream properties but different inflow strategies is the source of large uncertainties in the evaluation of the main quantities of engineering interest (as the skin friction coefficient distribution), which is still a major modeling bottleneck in hypersonic research.

From a computational perspective, a conservative approach to achieve an equilibrium state is to use very long computational domains [30],[31]. Experimental studies have also highlighted the need of taking flow measurements sufficiently far from the wind tunnel inlet section [11]. Recent works [35] have revealed that the streamwise length necessary to reach fully developed turbulence increases monotonically as the free-stream Mach number increases. Extending the analysis of Schlatter et al. [26], those authors considered fulfillment of the Von Karman equation, namely balance of friction and streamwise momentum flux as a quantitative criterion for the evaluation of the inflow length. Although their analysis was restricted to free-stream Mach number M_0 between 0.3 and 2.5, it may be expected that increasing trend is also valid at higher M_0, thus prompting new methods specifically tailored to minimize the development length.The current state-of-the-art modeling of inflow fluctuations is generally based on two classes of numerical methods: recycling-rescaling methods (RR) [17],[37] and digital filtering (DF) methods [16]. Quantitative evaluation of the performance of those methods is still lacking in supersonic/hypersonic flow, which based on the previous observations would be of great value. In this respect, introducing quantitative criteria for estimating the development length is a mandatory prerequisite.

We have carried out numerical simulations of supersonic SBLI in presence of crossflow, using the 2D/3C (two-dimensional, three-component) numerical approach previously employed by the research group for supersonic flow simulations and discussed by Di Renzo et al. [8]. A canonical two-dimensional SBLI, swept by an angle γ_0, is introduced into the computational domain, whose spanwise ends are orthogonal to the shock impingement line. Periodic boundary conditions are applied at the spanwise boundaries, which makes the configuration representative of a 3D swept SBLI (SSBLI) flow with cylindrical symmetry [32]. This configuration allows comparison both

Materials Research Proceedings 33 (2023) 388-396 https://doi.org/10.21741/9781644902677-57

with standard hypersonic boundary layers and with swept ones, at reduced computational cost as compared to fully three-dimensional simulations.

Regarding the assessment of inflow condition for supersonic boundary layers, a series of DNS have been carried out to analyze the spatial development of turbulence, using the data of Pirozzoli & Bernardini [22] as a benchmark. As previously mentioned, two goals are pursued: first, identifying suitable criteria to evaluate turbulence development towards an equilibrium state, and second look for modifications of the standard RR and DF techniques, in the attempt of overcoming their weaknesses.

Methodology

The analysis presented in this abstract relies on the numerical solution of the conservation equations for mass, momentum, and energy of a compressible fluid, which read:

$$\frac{\partial \rho}{\partial t} + \nabla \cdot (\rho \boldsymbol{u}) = 0$$
$$\frac{\partial (\rho \boldsymbol{u})}{\partial t} + \nabla \cdot (\rho \boldsymbol{u} \otimes \boldsymbol{u}) = -\nabla P + \nabla \cdot \underline{\underline{\boldsymbol{\tau}}}$$
$$\frac{\partial (\rho e_0)}{\partial t} + \nabla \cdot (\rho e_0 \boldsymbol{u}) = \nabla \cdot \left(\underline{\underline{\boldsymbol{\tau}}} \boldsymbol{u} + \lambda \nabla T + P \boldsymbol{u} \right).$$

In this formulation, ρ, P, and T are the density, pressure, and temperature of the gas, respectively, and **u** is the flow velocity vector field. The total energy per unit of mass of the gas is defined as $e_0 = e + u^2/2$, where $e = 1/(\gamma_g - 1)\,RT$ is the internal energy of the mixture per unit of mass, $\gamma_g = 1.4$ is the ratio of the heat capacities of the gas, R is the gas constant. The system of equations is complemented with the ideal gas equation of state

$$P = \rho R T$$

The local shear stress of the fluid is computed with the relation

$$\underline{\underline{\boldsymbol{\tau}}} = \mu \left[\nabla \boldsymbol{u} + \nabla u^T + 2(\nabla \cdot \boldsymbol{u})\, \underline{\underline{\boldsymbol{I}}}/3 \right]$$

where μ is the local dynamic viscosity of the mixture, evaluated using a power law of the type $\mu/\mu_0 = (T/T_0)^{0.76}$, whereas the thermal conductivity λ is computed using a constant Prandtl number $Pr = 0.72$.

The Navier-Stokes equations are solved using the in-house high-fidelity code STREAmS [4] for direct numerical simulations of compressible wall-bounded flows. The convective fluxes are discretized by means of a hybrid scheme which combines the energy-preserving properties of a sixth order skew-symmetric central difference scheme [20] with the shock-capturing properties of a fifth order weighted essentially non-oscillatory (WENO) scheme. The switch between the two methods is controlled by a modified Ducros sensor

$$\Theta = \frac{(\nabla \cdot \boldsymbol{u})^2}{(\nabla \cdot \boldsymbol{u})^2 + (\nabla \times \boldsymbol{u})^2 + (u_0/\delta_0)^2}$$

which is activated when $\Theta > 0.5$ in any point of the WENO stencil. The diffusive fluxes are discretized with sixth order central formulas, and the time advancement is carried out with a low-storage third order Runge-Kutta scheme [36].

Materials Research Proceedings 33 (2023) 388-396 https://doi.org/10.21741/9781644902677-57

SBLI setup

A schematic of the flow under scrutiny for the swept SBLI numerical campaign is provided in Figure 1. A turbulent boundary layer with thickness δ_0 is injected at the left boundary of the computational domain ($x/\delta_0 = 0$), and it develops over the bottom wall swept by an angle γ_0 with respect to the positive x direction. An oblique shock spanning the z direction impinges the boundary layer with an angle β with respect to the flat plate. The velocity inflow condition is obtained as a combination of a Van Driest-transformed incompressible Musker profile for the time-averaged field and velocity fluctuations obtained from a plane in x_r using a recycling-rescaling approach [17] suitable for compressible flows. The temperature fluctuation field is obtained from the streamwise velocity one using the strong Reynolds analogy (SRA).

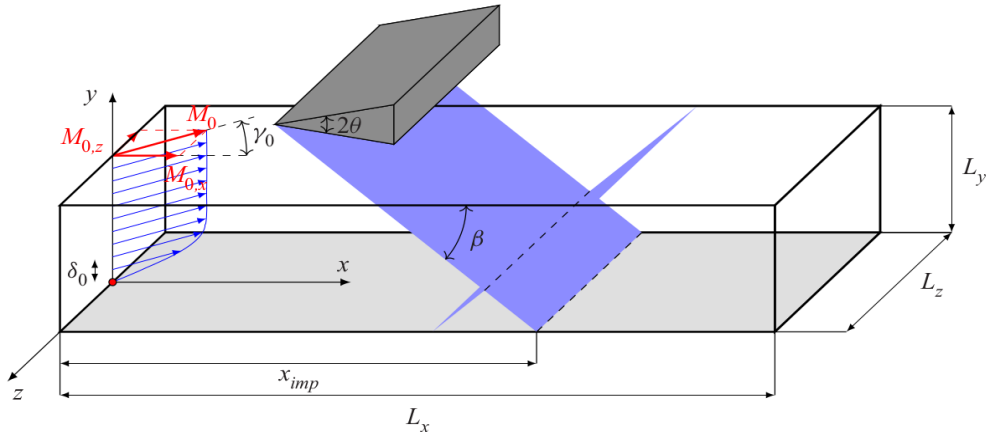

Figure 1. Schematic of SBLI setup: γ_0 is the incoming flow skew angle; δ_0 is the incoming boundary layer thickness; β is the shock angle, θ is the flow deflection angle and x_{imp} is the nominal location of the shock impingement (Figure from Ceci et al. [6], Creative Common license http://creativecommons.org/licenses/by/4.0/)

The bottom wall is assumed to be isothermal, and the wall temperature is set to its nominal turbulent recovery value for the incoming boundary layer (i.e. T_w/T_r=1, where $T_r/T_0 = 1 + r\,(\gamma_g - 1)/2\,M_0^2$ is the recovery to free-stream temperature ratio, $r = Pr^{1/3}$ is the recovery factor and Pr = 0.72 the Prandtl number). Periodicity of the flow is assumed in the z direction. Non-reflecting boundary conditions are imposed at the inlet and outlet boundaries to minimize numerical feedback. Nonreflecting boundary conditions are also used at the top boundary, except for a narrow zone where the incoming shock is injected into the computational domain by hard enforcement of the Rankine-Hugoniot jump relations. Various values of the inflow skew angle γ_0 and shock generator θ are considered. Extensive flow separation occurs for all the cases under investigation. Table 1 contains the key computational parameters of the simulation campaign.

Table 1. Summary of the SBLI flow cases

Case Label	M_0	M_{0x}	γ_0 (deg.)	θ (deg.)	$Re_{\delta 0}$	$(L_x \times L_y \times L_z)/\delta_0$	x_r/δ_0	x_{imp}/δ_0	T_w/T_r
G00_T08	2.28	2.28	0	8	15800	96 × 20 × 96	30	64	1
G00_T10	2.28	2.28	0	10.4	15800	96 × 20 × 96	30	64	1
G07_T10	2.3	2.28	7.5	10.4	15800	96 × 20 × 96	30	64	1
G15_T10	2.36	2.28	15	10.4	16200	96 × 20 × 96	30	64	1
G30_T08	2.63	2.28	30	8	19000	96 × 20 × 96	30	64	1
G30_T09	2.63	2.28	30	9.2	19000	96 × 20 × 96	30	64	1
G30_T10	2.63	2.28	30	10.4	19000	96 × 20 × 96	30	64	1
G45_T10	3.22	2.28	45	10.4	27500	96 × 20 × 96	30	64	1

Materials Research Proceedings 33 (2023) 388-396 https://doi.org/10.21741/9781644902677-57

Turbulent boundary layer (TBL) setup

The performance evaluation of standard turbulent inflow conditions for the DNS of supersonic/hypersonic turbulent boundary layers and the development of new inflow methods have been carried out with reference to the computational case of Pirozzoli & Bernardini [22] and Zhang et al. [38]. The first studied a spatially developing, supersonic zero-pressure-gradient (ZPG) boundary layer on a flat plate, with free-stream Mach number M_0=2 and nominally adiabatic wall conditions (T_w/T_r =1); the latter a spatially developing, ZPG hypersonic boundary layer at M_0=5.84 and cooled walls (T_w/T_r =0.25).

A series of direct numerical simulations has been performed, using several inflow conditions based both on recycling-rescaling (RR) and digital filtering (DF). A schematic representation of the recycling-rescaling setup is shown in Figure 2.

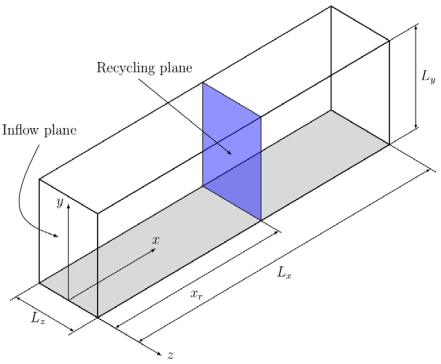

Figure 2. Set-up for recycling/rescaling: x_r denotes the position of the recycling plane, and L_x, L_y and L_z denote the size of the computational box (Figure from Ceci et al. [5], Creative Common license http://creativecommons.org/licenses/by/4.0/)

Standard recycling-rescaling and digital filtering inflow generations have been already implemented in the publicly available version of the STREAmS solver. Those routines have been modified throughout the course of the present project to test two novel inflow conditions. The flow is assumed to be periodic in the z direction, and non-reflecting boundary conditions are imposed on both the top and right boundaries. Time-averaging has been obtained by collecting instantaneous data for at least 800 convective time units δ_0/U_0; spanwise-averaging of the velocity and pressure fields is also performed. The list of DNS and the key computational setup are reported in Table 2.

Table 2. Summary of TBL flow cases

Flow Case	M_0	$Re_{\delta 0}$	$(L_x \times L_y \times L_z)/\delta_0$	x_r/δ_0	T_w/T_r
M2-RR	2	12662	106 × 8.3 × 9.6	53	1
M2-DF	2	12662	159 × 8.3 × 9.6	-	1
M2-L1	2	4479	310 × 26 × 32	53	1
M2-L2	2	8230	310 × 26 × 26	53	1
M2-L3	2	12662	318 × 16.6 × 19.2	53	1
M5.84-RR	5.84	23152	150 × 10 × 9	53	0.25
M5.84-DF	5.84	23152	150 × 10 × 9	-	0.25
M5.84-L1	5.84	10650	300 × 20 × 18	53	0.25
M5.84-L2	5.84	16788	300 × 20 × 18	53	0.25
M5.84-L3	5.84	23152	300 × 20 × 18	53	0.25

Materials Research Proceedings 33 (2023) 388-396 https://doi.org/10.21741/9781644902677-57

Results of the supersonic SBLI study

We have developed a simple model to characterize low-frequency unsteadiness in swept SBLIs, which is robustly supported from analysis of DNS data. We provide a scaling law for the spanwise undulation of the separation line and for the convection velocity of pressure disturbances, which concur to predict growth of the typical pressure oscillation frequency with the skew angle, consistent with trends observed in DNS. The proposed behavior of pressure fluctuations along the shock foot is described as

$$St_L = \left| St_{L,0} \pm \frac{\eta \, tan(\gamma_0)}{\alpha} \right|$$

with $\alpha \approx 2$ and $\eta \approx 0.7$, as obtained from the SBLI study, and $St_{L,0} \approx 0.04$.

Quantitative comparison of the numerically computed peak frequencies with the above prediction is presented in Figure 3. The prediction is clearly quite good, perhaps with exception of the single data point corresponding to $\gamma_0 = 30^\circ$, $\theta = 8^\circ$, which has a small separation bubble. Overall, the agreement becomes more satisfactory as the sweep angle increases [6].

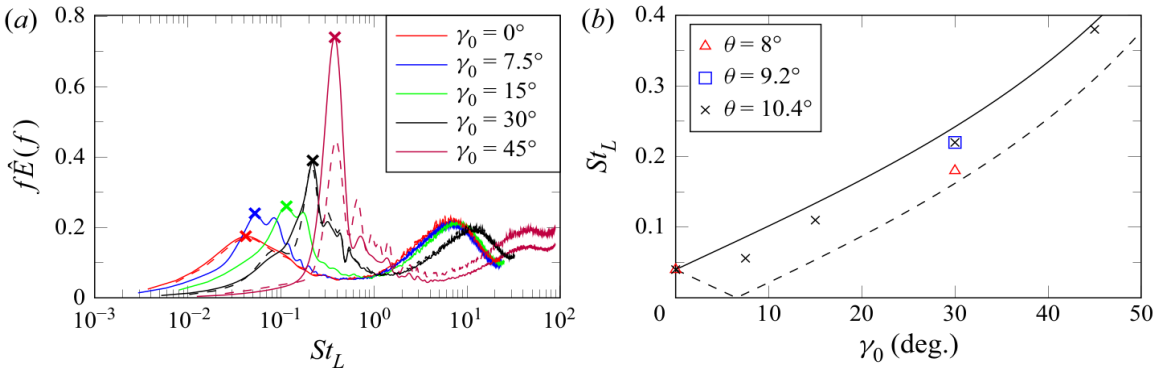

Figure 3: (a) Pre-multiplied normalized frequency spectra of wall pressure at the mean separation line for various sweep angles and for fixed shock strength ($\theta = 10.4^\circ$). Peaks are marked with crosses. Solid lines denote PSD obtained with the full-time window, whereas dashed lines denote PSD obtained with 50 % shorter time windows. (b) Peak frequency as a function of sweep angle: the solid and dashed lines denote the proposed prediction (Figure from Ceci et al. [6], Creative Common license http://creativecommons.org/licenses/by/4.0/).

Results of the TBL numerical tripping

Two reference flow cases have been selected, one representative of supersonic adiabatic boundary layers and the other of hypersonic cooled boundary layers. For both flow cases, two series of DNS have been carried out, one on relatively short domains, which serve to quantify effects of inflow seeding (RR- or DF-type), as compared to benchmark simulations, carried out in very long domains, which are verified to be yield to a healthy state of developed turbulence. The supersonic data set includes six DNS in short domains and three DNS in long domains, while the hypersonic data set includes four DNS in short domains, and three DNS in long domains.

We have derived a procedure to assess the TBL equilibrium conditions in numerical simulation by monitoring the deviation of significant metrics from a reference trend. Such metrics are the friction coefficient, wall pressure root mean square, Reynolds stress peaks and Stanton number [5]. In this respect, no single criterion can be used to define the inflow length for arbitrary flow conditions, but rather different metrics suggest different inflow adaptation lengths, which can also change as a result of the flow conditions. We have found that the friction coefficient is particularly sensitive to inflow seeding, and it can bear memory of inflow seeding quite far from the inflow plane [5].

References

[1]Adler, M. C. & Gaitonde, D. V. 2018 Dynamic linear response of a shock/turbulent-boundary-layer interaction using constrained perturbations. Journal of Fluid Mechanics 840. https://doi.org/10.1017/jfm.2018.70

[2]Adler, M. C. & Gaitonde, D. V. 2019 Flow similarity in strong swept-shock/ turbulent-boundary-layer interactions. AIAA Journal 57. https://doi.org/10.2514/1.J057534

[3]Babinsky, H. & Harvey, J. K. 2011 Shock wave-boundary-layer interactions. Cambridge University Press. https://doi.org/10.1017/CBO9780511842757

[4]Bernardini, M., Modesti, D., Salvadore, F. & Pirozzoli, S. 2021 Streams: A high-fidelity accelerated solver for direct numerical simulation of compressible turbulent flows. Computer Physics Communications 263, 107906. https://doi.org/10.1016/j.cpc.2021.107906

[5]Ceci , A., Palumbo , A., Larsson , J. & Pirozzoli , S. 2022 Numerical tripping of high-speed turbulent boundary layers. Theoretical and Computational Fluid Dynamics 36. https://doi.org/10.1007/s00162-022-00623-0

[6]Ceci , A., Palumbo , A., Larsson , J. & Pirozzoli , S. 2023 On low-frequency unsteadiness in swept shock wave-boundary layer interactions. Journal of Fluid Mechanics 956. https://doi.org/10.1017/jfm.2023.2

[7]Dhamankar, N. S., Blaisdell, G. A. & Lyrintzis, A. S. 2018 Overview of turbulent inflow boundary conditions for large-eddy simulations. AIAA Journal 56. https://doi.org/10.2514/1.J055528

[8]Di Renzo, M., Oberoi, N., Larsson, J. & Pirozzoli, S. 2021 Crossflow effects on shock wave/turbulent boundary layer interactions. Theoretical and Computational Fluid Dynamics. https://doi.org/10.1007/s00162-021-00574-y

[9]Dolling, D. S. 2001 Fifty years of shock-wave/boundary-layer interaction research: What next? AIAA Journal 39. https://doi.org/10.2514/3.14896

[10]Erengil, M. E. & Dolling, D. S. 1993 Effects of sweepback on unsteady separation in mach 5 compression ramp interactions. AIAA Journal 31. https://doi.org/10.2514/3.60176

[11]Erm, L. P. & Joubert, P. N. 1991 Low-reynolds-number turbulent boundary layers. Journal of Fluid Mechanics 230. https://doi.org/10.1017/S0022112091000691

[12]Fang, J., Yao, Y., Zheltovodov, A. A. & Lu, L. 2017 Investigation of Three-Dimensional ShockWave/Turbulent-Boundary-Layer Interaction Initiated by a Single Fin. AIAA Journal 55. https://doi.org/10.2514/1.J055283

[13]Gaitonde, D. V. 2015 Progress in shock wave/boundary layer interactions. Progress in Aerospace Sciences 72. https://doi.org/10.1016/j.paerosci.2014.09.002

[14]Gaitonde, D. V., Shang, J. S., Garrison, T. J., Zheltovodov, A. A. & Maksimov, A. I. 1999 Three-dimensional turbulent interactions caused by asymmetric crossing-shock configurations. AIAA journal 37. https://doi.org/10.2514/2.660

[15]Gross, A. & Fasel, H. F. 2016 Numerical investigation of shock boundary-layer interactions. In 54th AIAA Aerospace Sciences Meeting. https://doi.org/10.2514/6.2016-0347

[16]Klein, M., Sadiki, A. & Janicka, J. 2003 A digital filter based generation of inflow data for spatially developing direct numerical or large eddy simulations. Journal of Computational Physics 186. https://doi.org/10.1016/S0021-9991(03)00090-1

[17]Lund, T. S., Wu, X. & Squires, K. D. 1998 Generation of turbulent inflow data for spatially-developing boundary layer simulations. Journal of computational physics 140. https://doi.org/10.1006/jcph.1998.5882

[18]Padmanabhan, S., Maldonado, J. C., Threadgill, J. A. & Little, J. C. 2021 Experimental study of swept impinging oblique shock/boundary-layer interactions. AIAA journal 59. https://doi.org/10.2514/1.J058910

[19]Piponniau, S., Dussauge, J. P., Debiève, J. F. & Dupont, P. 2009 A simple model for low-frequency unsteadiness in shock-induced separation. Journal of Fluid Mechanics 629. https://doi.org/10.1017/S0022112009006417

[20]Pirozzoli, S. 2010 Generalized conservative approximations of split convective derivative operators. Journal of Computational Physics 229. https://doi.org/10.1016/j.jcp.2010.06.006

[21]Pirozzoli, S. & Bernardini, M. 2011a Direct numerical simulation database for impinging shock wave/turbulent boundary-layer interaction. AIAA Journal 49. https://doi.org/10.2514/1.J050901

[22]Pirozzoli, S. & Bernardini, M. 2011b Turbulence in supersonic boundary layers at moderate reynolds number. Journal of Fluid Mechanics 688. https://doi.org/10.1017/jfm.2011.368

[23]Pirozzoli, S., Bernardini, M. & Grasso, F. 2010 Direct numerical simulation of transonic shock/boundary layer interaction under conditions of incipient separation. Journal of Fluid Mechanics 657. https://doi.org/10.1017/S0022112010001710

[24]Pirozzoli, S. & Grasso, F. 2006 Direct numerical simulation of impinging shock wave/turbulent boundary layer interaction at M=2.25. Physics of Fluids 18. https://doi.org/10.1063/1.2216989

[25]Priebe, S. & Pino Martìn, M. 2012 Low-frequency unsteadiness in shock wave-turbulent boundary layer interaction. Journal of Fluid Mechanics 699. https://doi.org/10.1017/jfm.2011.560

[26]Schlatter, P., Li, Q., Brethouwer, G., Johansson, A. V. & Henningson, D. S. 2010 Simulations of spatially evolving turbulent boundary layers up to Reθ= 4300. International Journal of Heat and Fluid Flow 31. https://doi.org/10.1016/j.ijheatfluidflow.2009.12.011

[27]Schmisseur, J. D. & Dolling, D. S. 1994 Fluctuating wall pressures near separation in highly swept turbulent interactions. AIAA Journal 32. https://doi.org/10.2514/3.12114

[28]Settles, G. S., Perkins, J. J. & Bogdonoff, S. M. 1980 Investigation of three-dimensional shock/boundary-layer interactions at swept compression corners. AIAA Journal 18. https://doi.org/10.2514/3.50819

[29]Settles, G. S. & Teng, H. Y. 1984 Cylindrical and conical flow regimes of three-dimensional shock/boundary-layer interactions. AIAA Journal 22. https://doi.org/10.2514/3.8367

[30]Sillero, J. A., Jiménez, J. & Moser, R. D. 2013 One-point statistics for turbulent wall-bounded flows at reynolds numbers up to δ+ 2000. Physics of Fluids 25, 105102. https://doi.org/10.1063/1.4823831

[31]Simens, M. P., Jim´enez, J., Hoyas, S. & Mizuno, Y. 2009 A high-resolution code for turbulent boundary layers. Journal of Computational Physics 228. https://doi.org/10.1016/j.jcp.2009.02.031

[32]Threadgill, J. A. & Little, J. C. 2020 An inviscid analysis of swept oblique shock reflections. Journal of Fluid Mechanics 890. https://doi.org/10.1017/jfm.2020.117

[33]Vanstone, L. & Clemens, N. T. 2018 Pod analysis of unsteadiness mechanisms within a swept compression ramp shock-wave boundary-layer interaction at Mach 2. In AIAA Aerospace Sciences Meeting, 2018. https://doi.org/10.2514/6.2018-2073

[34]Vanstone, L., Musta, M. N., Seckin, S. & Clemens, N. T. 2018 Experimental study of the mean structure and quasi-conical scaling of a swept-compression-ramp interaction at Mach 2. Journal of Fluid Mechanics 841. https://doi.org/10.1017/jfm.2018.8

[35]Wenzel, C., Selent, B., Kloker, M. & Rist, U. 2018 DNS of compressible turbulent boundary layers and assessment of data/scaling-law quality. Journal of Fluid Mechanics 842, 428-468. https://doi.org/10.1017/jfm.2018.179

[36]Wray, A. A. 1990 Minimal storage time advancement schemes for spectral methods. Tech. Rep.NASA Ames Research Center, Moffett Field, CA.

[37]Xu, S. & Martin, M. P. 2004 Assessment of inflow boundary conditions for compressible turbulent boundary layers. Physics of Fluids 16. https://doi.org/10.1063/1.1758218

[38]Zhang, C., Duan, L., Choudhari, M.M. 2018 Direct numerical simulation database for supersonic and hypersonic turbulent boundary layers. AIAA J. 56(11), 4297-4311 https://doi.org/10.2514/1.J057296

[39]Zuo, F. Y., Memmolo, A., Huang, G. P. & Pirozzoli, S. 2019 Direct numerical simulation of conical shock wave-turbulent boundary layer interaction. Journal of Fluid Mechanics 877. https://doi.org/10.1017/jfm.2019.558